

# Absorption-based temperature-distribution-sensing for combustor diagnostics and control

Tudor I. Palaghita\* and Jerry M. Seitzman†  
*Georgia Institute of Technology,  
Daniel Guggenheim School of Aerospace Engineering,  
Atlanta, GA, 30332*

This paper describes the current development of a sensor for line-of-sight temperature distribution sensing in the exhaust of a combustor based on diode laser absorption. Temperature nonuniformity is characterized by defining a nonuniformity variable based on the difference in temperatures measured with two pairs of absorption lines. The nonuniformity variable  $U$  is shown to track the mixedness of the flow. Experimental measurements of temperature nonuniformity in a temperature-stratified combustor exhaust obtained with an external cavity diode laser system are shown. A sensor model is developed and used for error characterization and performance analysis. Simulations of sensor operation based on combustor temperature and concentration data from CFD simulations are used to analyze the problems encountered in the experiments. Laser tuning range and speed limitations are shown to be the major sensor performance limiting factors. The sensor concept is shown to work given appropriate hardware.

## I. Introduction

Gas turbine engines represent an area of particular interest to temperature measurement. Modern gas turbine engines require continuous improvements in performance, reduction in emission levels, and improved fuel flexibility and safety. Furthermore, engines need to become more intelligent and be able to adapt to changes during their operating life, such as aging, component upgrades, and new environmental restrictions. Improved control systems employed at all operating levels can provide solutions to many of these requirements. In particular, the development of temperature sensors, especially for the hot gas and reacting flow regions, can be a key enabler for many intelligent engine control systems.<sup>1-3</sup> Sensing becomes especially important at off-design operation and as engines age.

Understanding and being able to measure the gas temperature through different gas-turbine engine components can impact engine design, performance, lifetime, and cost. For example temperature fluctuations in the combustor may result in increased formation of  $\text{NO}_x$ , CO, and unburned hydrocarbons, which occur in pockets of hot gas.<sup>2,4,5</sup> Fluctuations of the combustor exhaust gas temperature in space and time also expose turbine blades and vanes to fluctuations in thermal stress, reducing safety and operability.<sup>1</sup> Furthermore, the ability to sense and limit the peak temperatures impinging on the turbine blades would permit less air to be diverted to cooling, thus increasing engine efficiency. The ability to sense and control the temperature profile at the combustor exit also allows increased average burning temperatures, which result in better engine performance and efficiency.<sup>2,5</sup> Fig. 1 schematically shows that for a given maximum

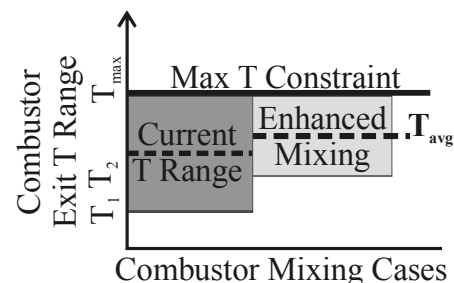


Figure 1. Reduced pattern factor enables higher average exit temperatures.

\*Graduate Research Assistant, School of Aerospace Engineering, AIAA Student member

†Associate Professor, School of Aerospace Engineering, AIAA Associate Fellow

© 2006 by T.I. Palaghita & J.M. Seitzman. Published by the American Institute of Aeronautics and Astronautics, Inc., with permission.

temperature constraint, a decrease in the amount of nonuniformity allows an engine designer to use higher average burning temperatures, thus increasing performance. As a result, understanding, measuring, and controlling the temperature distribution in the hot flow regions of gas-turbine engines emerges as a very important need, for both airborne and ground-based systems. Real-time monitoring of temperature uniformity also enables health monitoring of engine components, which is useful for lifetime predictions. Nevertheless, there are currently no practical, direct temperature nonuniformity sensors that can be used in operational gas-turbine engines.

This paper describes the continued development of a diode-laser, direct absorption sensor for line of sight temperature nonuniformity measurements across a combustor exit, or more generally through a region of hot gas. This sensor concept can be used for other applications, such as boundary layers, large arrays of industrial burners, and other industrial applications where temperature uniformity is essential for certain chemical processes.

The sensor functions by probing three or more water transitions with a diode laser; the ratio of absorbances of each pair of transitions yields a line-of-sight average temperature based on the Boltzman fraction of the absorbers. When the gas properties (temperature, absorber mole fraction) are uniform, any such pair would yield essentially the same temperature. When the gas properties change along the line of sight, because each line has a different nonlinear dependence on temperature and concentration, different line-pairs will yield different "average" temperatures. A nonuniformity parameter " $U$ " is defined based on two of these "average" temperatures.  $U$  approaches zero when the line-of-sight temperature is uniform and increases as it becomes more nonuniform.

Optical sensing is chosen because gas-turbine engines have stringent access, weight, and safety requirements. Diode lasers in particular, have proved extremely useful in the development of combustion sensors, as they are small, rugged, non-intrusive, fast, and can be used in conjunction with fiber-optics to locate the sensor remotely. Usually the laser is tuned over one or more spectral features and the resulting absorption is used to compute one or more flow properties of interest. Diode-laser sensors for average temperature, pressure, species concentration, and velocity based on absorption spectroscopy have been demonstrated for laboratory and in-situ combustion systems.<sup>6-10</sup> Previous work for temperature nonuniformity sensing<sup>11,12</sup> employed numerical simulation of water absorption with a broadband light source. It was shown that with three appropriately chosen absorption lines one can monitor for the presence of hot or cold spikes in the exhaust flow of a high-pressure combustor. A similar approach was later applied to measurements of  $O_2$  profiles in static heated cells of air.<sup>13</sup> Many closely spaced absorption lines were measured and used to compute the mole fraction or column-density of  $O_2$  corresponding to predefined temperature bins over the range of temperatures expected in the gas. This technique was named "temperature binning."<sup>13</sup>

Based on the previous discussion, an application of particular interest for an absorption based temperature sensor is circumferential pattern factor sensing and control in an annular combustion rig (Fig. 2). For example, using a few of these sensors, the whole circumferential temperature profile can be characterized (and therefore related issues such as nonuniformities between injectors, problems with specific injectors, and mixing issues) and controlled.

## II. Absorption theory

The narrowband absorption of a light signal at wavelength  $\nu$  ( $cm^{-1}$ ) with incident intensity  $I_0$  and transmitted intensity  $I$  by a medium of thickness  $L$  (cm), is described by the Beer-Lambert Law as:

$$\frac{I}{I_0}(\nu) = e^{\int_0^L -pxS_i(T)\phi(\nu-\nu_0, T, x, p)dl}, \quad (2)$$

where  $p$  is the pressure (atm),  $x$  is the absorber mole fraction,  $S$  is the line strength ( $cm^2 atm^{-1}$ ) of the  $i^{th}$  transition (centered at  $\nu_0$ ),  $T$  is the temperature (K), and  $\phi$  is the line shape function (cm) whose integral is normalized to unity. For simplicity we assume all measurements are done at the same instant in time. For a particular transition  $i$  centered at  $\nu_{0,i}$ , the line strength  $S$  is a function of temperature only:

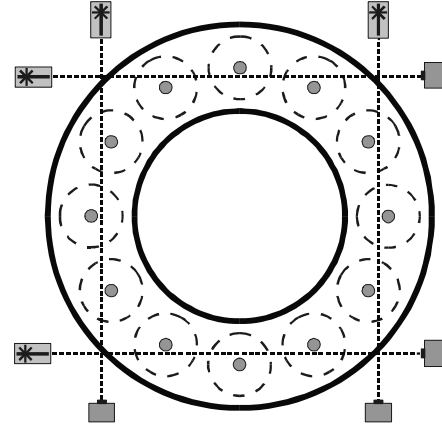


**Figure 2. Gas-turbine annular combustor exit plane instrumented for pattern factor sensing.**

$$S_i(T) \approx S_i(T_0) \frac{Q(T_0) T_0}{Q(T) T} \exp\left(-\frac{hcE''}{k} \left(\frac{1}{T} - \frac{1}{T_0}\right)\right), \quad (3)$$

where  $Q$  is the partition function,  $E''$  is the lower state energy of the transition ( $\text{cm}^{-1}$ ),  $h$  is Plank's constant,  $c$  is the speed of light, and  $k$  is Boltzman's constant.  $T_0$  is a reference temperature, taken here to be 296 K, consistent with the HITRAN database.<sup>14</sup>

### A. Uniform Flow Properties

In a medium with uniform properties (temperature and concentration), one can determine the temperature and mole fraction of the species of interest by probing two absorption lines. By integrating over a frequency band centered at  $\nu_0$ , the line shape function is eliminated and the temperature can be directly determined from the ratio of the absorbances  $abs$  of two lines ( $i$  and  $j$ ):

$$abs_i = \int_{-\infty}^{\infty} -\ln\left(\frac{I}{I_0}(\nu)\right) d\nu = \int_{-\infty}^{\infty} \int_0^L p \cdot x \cdot S_i(T) \phi_i(\nu - \nu_0, T, x, p) dl d\nu = px S_i(T) L \quad (4)$$

$$T_{ij} = \left[ \frac{1}{T_0} - \frac{1}{1.44(E_i - E_j)} \ln\left(\frac{abs_i S_{0j}}{abs_j S_{0i}}\right) \right]^{-1} \quad (5)$$

Using the absorbance of two lines, one can determine the temperature of the gas using Eq. (5) and the concentration of the species of interest using Eq. (4). In this gas with uniform properties, any two lines picked would yield the same results (neglecting experimental errors).

### B. Nonuniform Flow Properties

In a flow with spatial variations in temperature and species concentration, such as most practical combustion flows, the integral in Eq. (4) cannot be solved without prior knowledge of either the temperature or concentration profiles (we still assume steady flow or instantaneous measurements). For arbitrary temperature and concentration profiles along the line of sight, the absorbance of each line  $i$  becomes:

$$abs_i = \int_0^L x(l) S_i(T(l)) dl \quad (6)$$

As  $S(T(l))$  is a nonlinear function of temperature, a uniform profile with temperature  $T$  and a nonuniform one with an average temperature  $\bar{T} = T$  will have different  $\int_0^L S(T(l)) dl$  values (representing a nonlinear averaging process) and different absorbance values. This fact can be used to infer information about the temperatures along the line of sight.

The ratio of the absorbances of 2 lines  $i$  and  $j$  depends on the spatial distributions as well:

$$R_{ij} = \frac{abs_i}{abs_j} = \frac{\int_0^L x(l) S_i(T(l)) dl}{\int_0^L x(l) S_j(T(l)) dl}, \quad (7)$$

and is no longer a function of temperature only. This means that the ratio of the absorbances becomes a function of the two chosen lines (through their spectroscopic parameters having a different nonlinear dependence on  $T(l)$ ). Even for the case when the temperature changes along the line of sight but the concentration is uniform, the ratio in equation (7) is a nonlinearly path-weighted function of temperature, specific to the two lines  $i$  and  $j$ . Information about the temperature nonuniformity along the line of sight can thus be inferred from the information contained in measurements of several absorption lines or their ratios.

### III. Sensor Operating Principle

Using the above theory, we construct a simple sensor for temperature nonuniformity based on instantaneous measurements of three absorption lines. With the ratio of two lines, an ‘‘average’’ temperature  $T_{ij}$  is computed using equations (7) and (5), as illustrated in equation (8).  $T_{ij}$  is then computed by assuming uniform properties along the path (Eq. 4).

$$R_{ij} = \frac{abs_i}{abs_j} = \frac{\int_0^L x(l)S_i(T(l))dl}{\int_0^L x(l)S_j(T(l))dl} \xrightarrow{\text{define}} = \frac{S_i(T_{ij})}{S_j(T_{ij})} \quad (8)$$

$T_{ij}$  is not the actual average temperature, but a quantity that depends on the line-of-sight distribution of species mole fraction and temperature, as well as the spectroscopic properties of the two lines forming the ratio. The average temperature  $T_{ij}$  will depend on the chosen pair of lines  $i$  and  $j$  because each line has a different dependence on temperature. This result will also depend in great measure on the correlation between absorber concentration and temperature. Nevertheless, as long as the concentration-temperature relationship (correlation) does not change, the ratio remains a function of temperature only. Also, the more we know about how the mole fraction and temperature are related, the more meaningful  $T_{ij}$  becomes.

While no discrete spatial information can be obtained when using only one line-of-sight sensor, one can compute various ‘‘average’’ temperatures by measuring several pairs of lines. The absorption ratios of each pair of lines, say  $I&2$  and  $I&3$ , yield path-averaged temperatures,  $T_{12}$  and  $T_{13}$ . When the gas properties change along the line of sight, different line-pairs will yield different ‘‘average’’ temperatures. As the temperature profile becomes uniform, these temperatures ( $T_{ij}$ ) will converge to the same number, but if the profile is nonuniform, they will diverge. This fact is used to measure the degree of nonuniformity in the flow. The more lines one can measure, the more information can be inferred about the temperature distribution along the line of sight. For a simple sensor, two of these ‘‘average’’ temperatures are combined into a nonuniformity parameter ‘ $U$ ’ defined below:

$$U = \frac{|T_{12} - T_{13}|}{0.5 \cdot (T_{12} + T_{13})} = \frac{\Delta T}{\bar{T}} \quad (9)$$

This variable goes towards zero when the gas has uniform properties, and increases as the temperature nonuniformity increases or as the degree of mixing decreases.

To visually show the dependence of  $U$  on temperature nonuniformity, a measure of this nonuniformity (such as pattern factor) has to be defined that takes into account the magnitude of the temperature deviations from the mean as well as the spatial extent of these deviations. After considering the merits and shortcomings of several measures, a temperature profile factor ( $Tpf$ ) is defined using the RMS over the mean of the actual combustor exit temperature ( $T_4$ ) as a measure of its uniformity. The temperature profile factor is henceforth used in all plots.

$$Tpf = \frac{T_{4,rms}}{T_{4,average}} \quad (10)$$

For the current sensor setup, water is chosen as the marker species because it is a major combustion product that has relatively strong absorption lines throughout a large portion of the spectrum. Moreover, it is easy to find water lines with little or no interference from other combustion products.

To illustrate how this sensor works,  $U$  was computed for several simple temperature profiles with the same average temperature of 1500 K and small deviations from the mean of 10% and 20% in temperature spanning 5% and 10% of the path (Fig. 3). The path length was chosen as 20 cm and water concentration was set to be constant for this comparison. As the size and extent of the temperature deviations increases, as measured by the  $Tpf = T_{rms}/T_{avg}$  of the actual temperature profiles, so does  $U$ .

The sensor described above represents a basic configuration. This concept can be extended to several laser beams, each yielding such a measurement. A concept of the multiple-beam sensor was illustrated in Fig. 2.

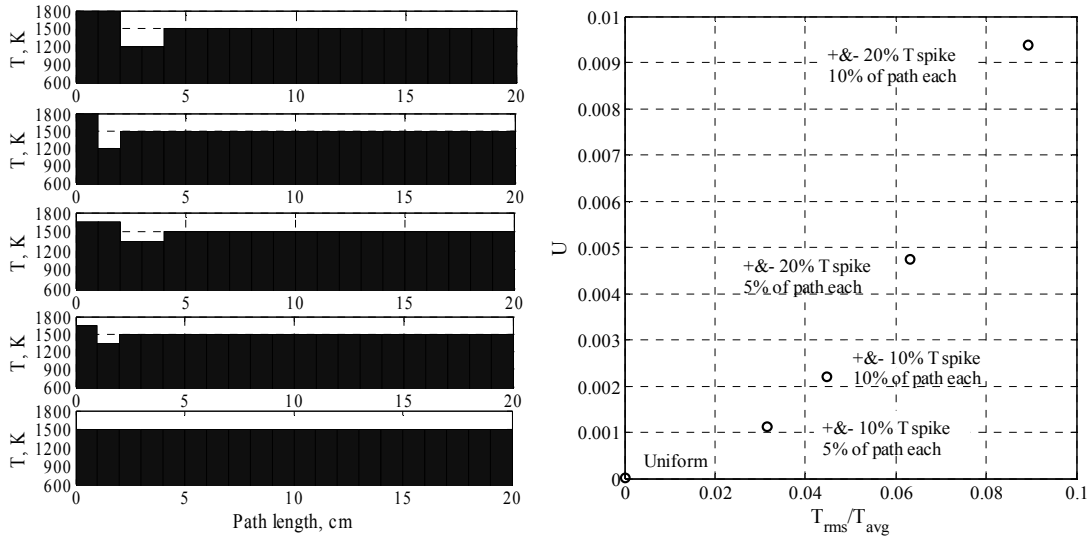


**Figure 3.**  $U$  values for several simulated temperature profiles with spikes of increasing magnitude and width. The water concentration was assumed constant.

#### IV. Experimental and Numerical Studies

A sensor based on the principles described above was implemented in the laboratory and tested in the exhaust of a temperature-stratified combustor. A computer model of the sensor was also built and used in conjunction with experiments to prove the sensor concept and analyze its performance and sensitivity to errors.

Initial experimental results have been presented previously<sup>15</sup> and demonstrate the feasibility of this sensing approach. Fig. 4 shows that for two different combustor conditions (obtained by changing the air and fuel flow rates) characterized by different exhaust temperature profiles, the measured nonuniformity parameter  $U$  is smaller for the more uniform temperature profile.

Further experimental studies were conducted in a test rig with higher exit temperatures (Fig. 5) and improved control of the exhaust temperature profile. Measurements in this modified setup yielded mixed results. In some tests (Fig. 6 left), the  $U$  parameter generally exhibited the expected trend, increasing with  $T_{rms}/T_{avg}$ . In other cases, there was a large scatter in  $U$  and poor correlation with the degree of temperature nonuniformity (Fig. 6 right). The possible causes of this scatter were identified and studied in order to redesign the sensor and decrease its sensitivity to errors.

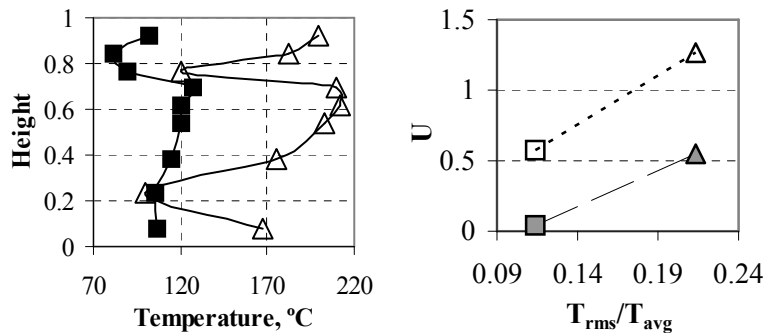


**Figure 4.** Combustor exit temperature profiles (left) for two operating settings and nonuniformity parameter  $U$  (right) based on two groups of absorption lines (dotted line and dashed line).

A numerical model of the sensor was built to study the sources of errors and to better understand their effects on sensor performance. A comparison between the physical sensor and the model is shown in Fig. 7. To make the model more realistic, line-of-sight temperature and species profiles are obtained from a Large Eddy Simulation model of a combustor.<sup>17</sup> The transmitted laser signal that would normally be detected in the combustor exhaust is obtained by calculating the path-averaged absorption for the given temperature and concentration profiles.

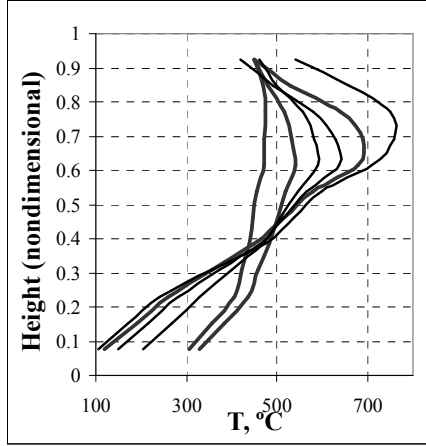


Figure 5. Typical combustor exit temperature profiles.

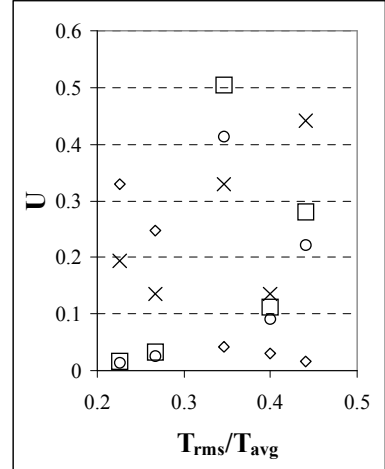
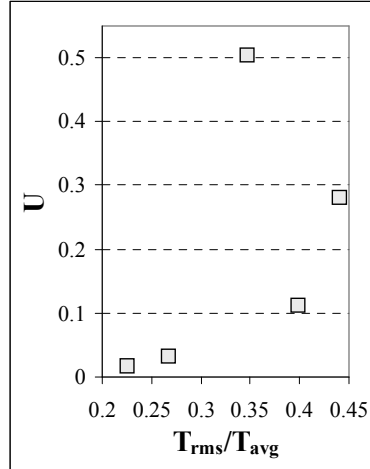


Figure 6. Measurements of  $U$  in the exit of a temperature stratified methane-air combustor.

The resulting simulated laser transmission scans are reduced with the same sensor data analysis software used in the experiments. The sources of errors and the laser output were also modeled and added to the detector signal. This analysis model is very useful in studying the sensitivity of the sensor to the different sources of errors and devise ways to minimize their effects. Furthermore, the model can be used to determine minimum laser and hardware specifications needed for a required level of sensor performance and optimize the sensor design. This model can also be used to design and test a temperature nonuniformity control system.

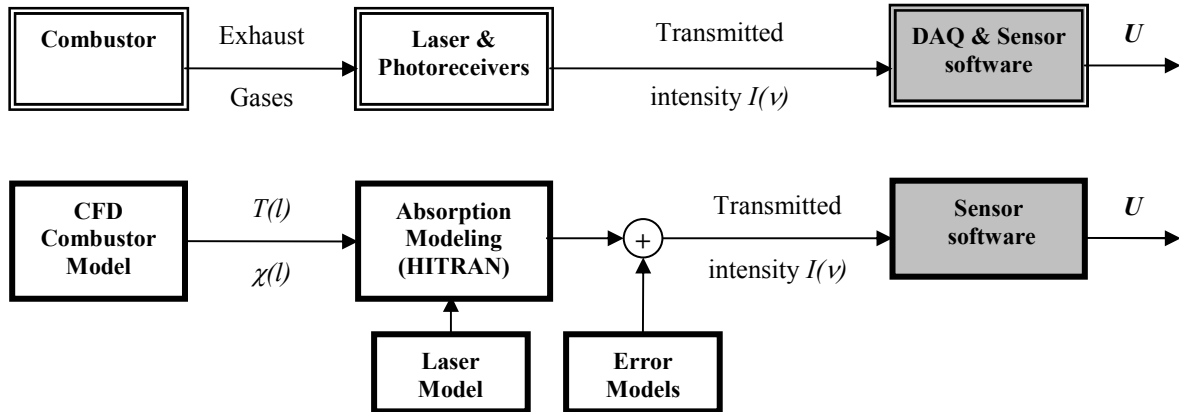


Figure 7. Physical sensor system and sensor analysis model using CFD data.

## V. Sensor Performance Analysis

The sensor performance depends on the hardware used and on designing the sensor to match the specific application (e.g appropriate choice of absorption lines, reduction of outside absorption, etc.). The choice of laser limits the available absorption lines that can be probed as well as the tuning speed. Lasers that can tune at very high rates (kHz to MHz) over several absorption features enable 2f spectroscopy techniques to be used instead of direct-absorption, greatly increasing noise rejection and baseline fitting errors. Furthermore the choice of absorption lines to be used has a very large impact on sensitivity. Ideally one wants absorption lines with large and very different response to changes in temperature in the expected range.

To qualify the results presented above, we briefly discuss the limitations due to the hardware used in these experiments and then describe the analysis of other error sources typical for these sensors. These limitations include slow tuning speed, which makes the sensor more sensitive to beam-steering and combustor unsteadiness, limited tuning range, which limits the sensor to measuring one line at a time and then slowly moving on to the next line, highly nonlinear laser power to wavelength output, and the inherent limitation in available water transitions within

the laser bandwidth. Besides these limitations, errors are introduced by combustor unsteadiness, possible changes in water-temperature correlation, absorption due to water in the air outside the combustor, and beam-steering.

### A. Hardware limitations

From an analysis of the experiment and the combustor characteristics it was determined that the scatter sometimes exhibited by the experimental results is mostly due to the limitations imposed by the available diode laser. Although there are new commercial lasers that have very good tuning characteristics (wider bandwidth – tenths of nm – and much faster tuning – in the MHz range), the experimental results presented here are limited by the narrow tuning range (over one water transition, or about 0.4nm) and low scan repetition speed (up to 140 Hz) of the available laser. These factors limit the measurements to consecutive averages of each absorption line, which means that each line might be measured at slightly different combustor conditions as a result of unsteadiness. These unsteadiness effects are reduced by averaging measurements taken over a long enough period of time (several seconds) to capture all combustor fluctuations. The resulting average absorbance and respective  $U$  values characterize the average combustor conditions at that operating setting. This method was proven effective through sensor simulations.<sup>16</sup>

Another limitation imposed by using the current laser is the inability to choose absorption lines that have a high sensitivity to changes in temperature in the range of our combustor. The water lines that can be probed with this laser have relatively low sensitivities to temperature changes, increasing the effects of errors.

Furthermore, the narrow tuning range and nonlinear laser power output as a function of wavelength makes fitting a baseline ( $I_0$ ) to the wings of the absorption line very difficult. This laser exhibits a highly nonlinear power vs. wavelength output with large etaloning effects. To obtain the absorbance, the laser baseline is fitted to the far wings of each absorption line (Fig.8). The narrow tuning range makes it very difficult to capture enough of the wings for a good baseline fit. Even small baseline fitting errors result in generally underestimated absorbances and large scatter of the  $U$  values. For example, after reexamining one experimental data set, it was determined that because of poor baseline fitting several absorption lines resulted in consistently low absorbance values (by more than 10%) – these are plotted in Fig. 9. An improvement of the laser baseline fitting for one of the 3 lines that form  $U$  reduces the scatter and moves one of the bad  $U$  points on the expected trend-line (Fig. 10). Additional improvements in the baseline fits for the other two lines reduce the scatter further, moving the remaining bad points close to the expected  $U$  trend-line (Fig. 12). Nevertheless, because the wings of these lines are not completely resolved, the computed absorbances are still too low. An arbitrary small (2-4%) correction in the absorbance values can push all  $U$  points on the expected trend-line. Errors and limitations in baseline fitting were determined to be the most significant sources of errors for this data set.

In a practical combustor operating at higher temperatures, it is easier to choose absorption lines with better sensitivity to temperature changes. Furthermore, a sensor implementation using a laser with better characteristics and probing better absorption lines at high temperatures will have much better error rejection, resulting in better tracking of nonuniformity.

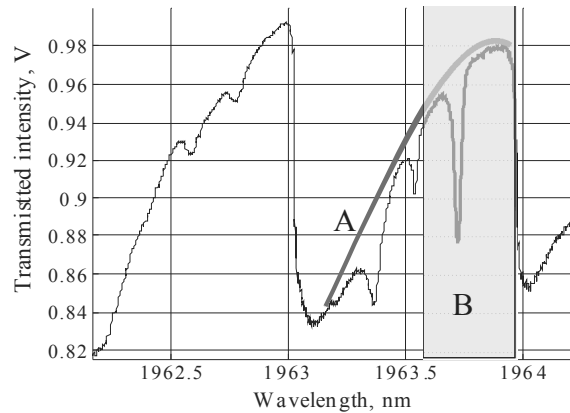


**Figure 8. Slow & wide laser scan. Small dips are absorption lines; large dips represent laser etalon effects. A – actual laser baseline  $I_0$ . B – fast tuning range.**

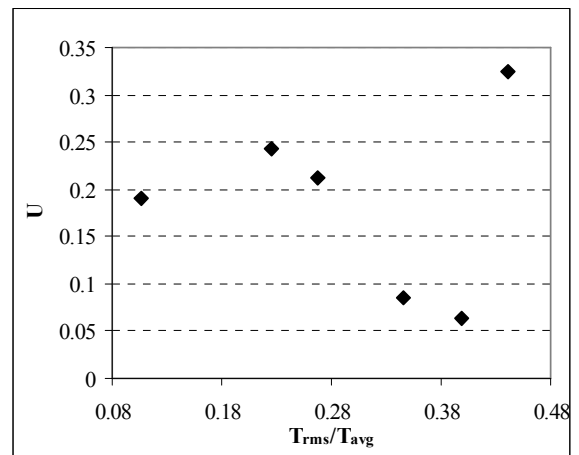


**Figure 9.  $U$  as a function of the temperature profile factor, before baseline corrections.**

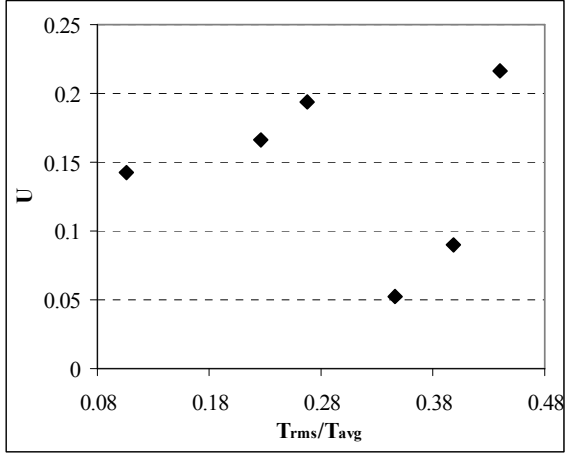


**Figure 10.**  $U$  as a function of the temperature profile factor, after baseline correction to one line.

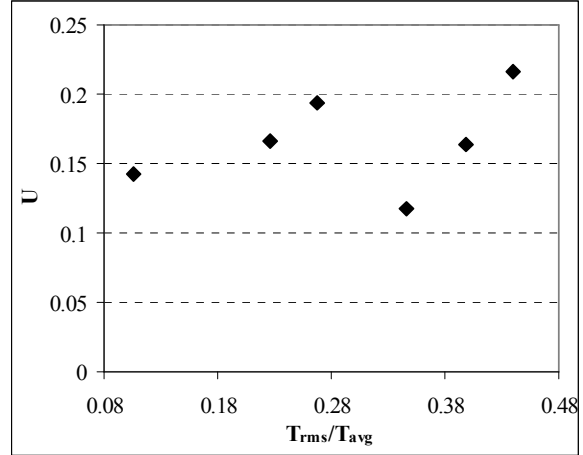


**Figure 12.**  $U$  as a function of the temperature profile factor, after baseline corrections to two lines.

Using the sensor model described above, we study the effects of systematic and random errors in the laser baseline fitting. Using the measured temperature profiles corresponding to the  $T_{pf}$  used in the above figures and the same absorption lines, we compute and plot  $U$  for several cases (Fig. 11). The error free case is represented by circles. First, a random error is introduced at each baseline fit, corresponding to 0-4% underestimation of each absorbance (crosses). Then it is assumed that each line will have a similar baseline error for all conditions (T profiles) resulting in the same percentage absorbance error – different lines have different fit errors. Two cases are presented (triangles) – the expected  $U$  trend is maintained in one, in another it is not. Although this is not an accurate representation of the actual fitting errors, this simple model proves that even these small errors have an effect of the same magnitude as the scatter in the experimental data. Further study also shows that if all baseline fits are biased in a similar manner, the increasing trend of  $U$  with the  $T_{pf}$  is not significantly affected. These types of baseline fitting errors are the only errors shown to affect the resulting  $U$  values on a scale similar to the experiments.

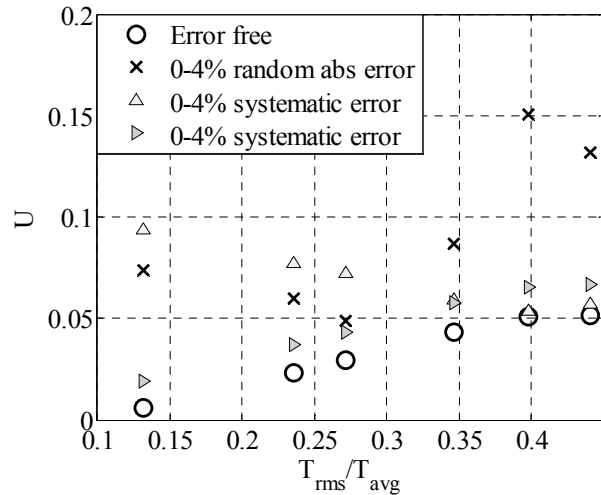


**Figure 11.**  $U$  with baseline fitting errors.

## B. Experimental sources of errors

Besides the laser imposed limitations, all such sensors are prone to other experimental errors. In practical applications random noise or other symmetric-type errors (unsteadiness, turbulence) do not significantly affect sensor performance because measurements are averaged over time.

Non-symmetric errors can not be eliminated through averaging. For example, the baseline fitting errors described above are biased errors, as they always results in underestimation of the absorbance values. Another source of biased errors is beam-steering, which always results in smaller absorbance values. Beam steering may introduce significant errors by moving the laser beam off the detector as a result of changes in the index of refraction along the line of sight. Usually this can be mitigated by scanning at high speeds and essentially freezing the flow during a line scan. With the current laser scanning at 140Hz, beam steering effects are diminished by discarding all line traces that exhibit significant signal losses or are significantly skewed away from a Voigt profile.

Sometimes the physics of the problem and not the experimental technique may be the source of errors. For example, another possible reason for the scatter in measured  $U$  values might be the changing correlation between water and temperature due to wall cooling in the test combustor. Any absorption sensor is affected both by the temperature field and the concentration field. If the temperature and concentration are correlated and the correlation

never changes, it is equivalent to saying that the concentration is a set function of temperature, so that  $U$  will still be a measure of changes in the temperature profile only. When this correlation changes,  $U$  becomes a composite measure of changes in the temperature field combined with “independent” changes in the concentration field. In most practical gas-turbine combustors the temperature and species concentrations are directly correlated (i.e. hotter regions have more water), regardless of operating conditions. Also, heat losses at the walls are relatively small.

To investigate the effect of changes in correlation on  $U$ , we use the measured combustor exit temperatures (Fig. 5) and simulate the sensor operation for several water distributions at every operating condition. For example, for a given temperature profile characterized by a  $T_{rms}/T_{avg}$  value, we compute  $U$  for constant water, for water linearly dependent on temperature, quadratic, and several random water distributions with the same mean, some of them extreme. The resulting  $U$  values for each operating condition ( $T_{rms}/T_{avg}$ ) are shown in Fig. 13. Although there is some scatter, especially in the more nonuniform cases, the  $U$  values still increase overall. Furthermore, the  $U$  values and their scatter in these simulations are much smaller than the measured ones. Also small changes in correlation have a small effect on  $U$ . This suggests that the changing correlation is not a major problem and there are other factors, such as the inability to fast-tune the laser over several lines that have a larger contribution to the errors observed in the measured  $U$  values.

In conclusion, experimental errors were determined to be relatively small compared to errors stemming from hardware limitations. These types of experimental errors can be further reduced through averaging and rapid tuning, or use of 2f techniques. The major limitation to increasing the sensitivity of the sensor and its repeatability is the current laser, through the errors or inability to measure the baseline signal, as well as the limited tuning range and speed.

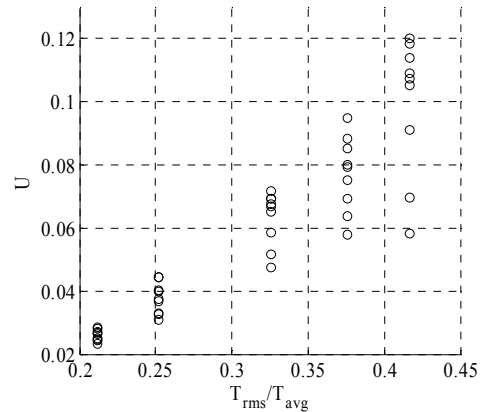


**Figure 13.  $U$  for several correlations between temperature and concentration.**

## VI. Conclusions

The ongoing development of a sensor that can characterize the line of sight temperature distribution in the exhaust of a combustor or through any region of hot flue gases has been presented. The sensor works by measuring three absorption lines, and computing a nonuniformity parameter  $U$  based on the three absorbances. Experimental testing and sensor simulations have demonstrated the ability of  $U$  to generally track changes in the shape of the temperature profile in the exhaust of a combustor. Limitations of the current hardware sometimes result in large errors in the  $U$  parameter. A sensor model was developed and used to investigate and quantify the effects of hardware and other experimental errors on the sensor performance. It was determined that laser tuning range and speed were the primary sources of errors, while the effects of combustor unsteadiness, variations in water-temperature correlation, and general noise can be reduced through use of modern hardware, averaging and sensor design. Sensor simulations also showed that given better, commercially available lasers, errors expected in practical implementations of this sensor can be easily overcome.

In conclusion, a sensor that can characterize the line of sight temperature distribution in the exhaust of a combustor was described and analyzed through experimental tests and computer simulations.

## VII. Acknowledgments

This research was supported by NASA through the University Research, Engineering, and Technology Institute for Aeropropulsion and Power, under Grant/Cooperative agreement NCC3-982.

## VIII. References

- <sup>1</sup> Kiel, Barry, “Review Of Advances In Combustion Control, Actuation, Sensing, Modeling And Related Technologies For Air Breathing Gas Turbines,” AIAA Paper 2001-0481, 39\* *AIAA Aerospace Sciences Meeting and Exhibit*, Reno, NV, Jan 8-11, 2001.
- <sup>2</sup> Lord, W. K., MacMartin, D.G., Tillman, G., “Flow Control Opportunities In Gas Turbine Engines,” AIAA Paper 2000-2234, *Fluids 2000*, Denver, CO, June 19-22, 2000.
- <sup>3</sup> Garg, Sanjay, “Propulsion Controls and Health Management Research at NASA Glenn Research Center,” *NASA Report TM-2002-211590*, 2002.

- <sup>4</sup> McCarty, B, Tomond, C, and McGinley, R, "Reliable and Affordable Control Systems Active Combustor Pattern Factor Control," *NASA Technical Report NASA CR—2004-213097* 21–11165, July 2004.
- <sup>5</sup> DeLaat, John C. et al., "Active Combustion Control for Aircraft Gas Turbine Engines," AIAA paper 2000-3500, *Joint Propulsion Conference and Exhibit*, 36th, Huntsville, AL, July 17-19, 2000.
- <sup>6</sup> Teichert, H., Fernholz, T., and Ebert V., "Simultaneous in situ measurement of CO, H<sub>2</sub>O, and gas temperatures in a full-sized coal-fired power plant by near-infrared diode lasers," *Applied Optics*, Vol. 42, No. 1220, April 2003, pp. 2043-2051.
- <sup>7</sup> Allen, M.G., "REVIEW ARTICLE: Diode laser absorption sensors for gas-dynamic and combustion flows," *Measurement Science and Technology*, Vol. 9, 1998, pp. 545–562.
- <sup>8</sup> Zhou, X., Liu, X., Jeffries, J.B., and Hanson R.K., "Development of a sensor for temperature and water concentration in combustion gases using a single tunable diode laser," *Measurement Science and Technology*, Vol. 14, 2003, pp. 1459–1468.
- <sup>9</sup> Mihalcea, R.M., Baer, D.S., Hanson, R.K., "Diode-laser absorption measurements of CO<sub>2</sub> near 2 μm at elevated temperatures," *Applied Optics*, Vol. 37, No. 36, 20 December 1998, pp. 8341-8347.
- <sup>10</sup> Nagali, V. and Hanson, R.K., "Design of a diode-laser sensor to monitor water vapor in high-pressure combustion gases," *Applied Optics*, Vol. 36, No. 36, 20 December 1997, pp. 9518-9527.
- <sup>11</sup> Seitzman, J.M. and Scully, B.T., "Broadband infrared absorption sensor for high-pressure combustion control," *Journal of Propulsion and Power*, Vol. 16, No. 6, pp. 994-1001, 2000.
- <sup>12</sup> Seitzman, J.M., Tamma, R., and Scully, B., "Broadband infrared sensor for active control of high pressure combustors," AIAA Paper 98-0401, *Aerospace Sciences Meeting & Exhibit*, 36th, Reno, NV, Jan. 12-15, 1998.
- <sup>13</sup> Sanders, S.T., Wang, J., Jeffries, J.B., and Hanson, R.K., "Diode-laser absorption sensor for line-of-sight gas temperature distributions," *Applied Optics*, Vol. 40, No. 24, 20 August 2001, pp. 4404-4415.
- <sup>14</sup> Rothmana, L.S., Barbeb, A., Chris Bennerc, D., Brownd, L.R., Camy-Peyrete, C., Carleerf, M.R., Chancea, K., Clerbauxf, C., Danae, V., Devic, V.M., Fayth, A., Flaudi, J.M., Gamachej, R.R., Goldmank, A., Jacquemarta, D., Jucksa, K.W., Laffertyl, W.J., Mandine, J.-Y., Massiem, S.T., Nemtchinovn, V., Newnhamo, D.A., Perrini, A., Rinslandp, C.P., Schroederq, J., Smitho, K.M., Smithp, M.A.H., Tangq, K., Tothd, R.A., Vander Auweraf, J., Varanasin, P., Yoshinoa, K., "The HITRAN molecular spectroscopic database: edition of 2000 including updates through 2001," *Journal of Quantitative Spectroscopy & Radiative Transfer*, Vol. 82, 2003, pp. 5–44.
- <sup>15</sup> Palaghita, T. and Seitzman, J. M., "Control of temperature nonuniformity based on line-of-sight absorption," AIAA Paper 2004-4163, *AIAA/ASME/SAE/ASEE Joint Propulsion Conference and Exhibit, 40<sup>th</sup>*, Fort Lauderdale, FL, 11 - 14 Jul 2004.
- <sup>16</sup> Palaghita, T. and Seitzman, J. M., "Pattern Factor Sensing and Control Based on Diode Laser Absorption," AIAA Paper 2005-3578, *AIAA/ASME/SAE/ASEE Joint Propulsion Conference and Exhibit, 41<sup>st</sup>*, Tucson, AZ, 11 - 13 Jul 2005.
- <sup>17</sup> Eggenpieler, G. and Menon, S., "Parallel Numerical Simulation of Flame Extinction and Flame Lift-Off," Proceedings of the *Parallel Computational Fluid Dynamic Conference*, Washington, DC, May 24-27, 2005